Supplementary Information

Global intraurban intake fractions for primary air pollutants from vehicles and other distributed sources

Joshua S. Apte [a], Emilie Bombrun [b], Julian D. Marshall [b,*], and William W Nazaroff [c]

[a] Energy and Resources Group, University of California, Berkeley, CA, 94720-3050 USA

[b] Department of Civil Engineering, University of Minnesota, Minneapolis, MN 55455-0233 USA

[c] Department of Civil and Environmental Engineering, University of California, Berkeley, CA, 94720-1710 USA

Contents

Pages: 21
Figures: 10
Tables: 9

[*] Corresponding author. E-mail: julian@umn.edu. Phone: 612-625-2397. Fax: 612-626-7750. Address: 500 Pillsbury Drive SE, University of Minnesota, Minneapolis MN 55455-0233 USA

SI.1 Methods

SI.1.1 Vertical wind profile

MERRA data provide wind speed at a standard 10-meter height. We use the following truncated power-law relationship to evaluate wind speed at a specific time ($u(z,t)$; units: m s^{-1}) as a function of height (z, units: m).[1-3]

$$u(z,t) = u_{\mathrm{ref}}(t) \times \left(\frac{z}{H_{\mathrm{ref}}}\right)^p \quad \text{for } z \leq H_{\max} \qquad \text{SI.1a}$$

$$u(z,t) = \text{constant} = u_{\mathrm{ref}}(t) \times \left(\frac{H_{\max}}{H_{\mathrm{ref}}}\right)^p \quad \text{for } z > H_{\max} \qquad \text{SI.1b}$$

Here, $u_{\mathrm{ref}}(t)$ is the wind speed (m s^{-1}) at the reference height at a specific time, H_{ref} is the reference height (10 m), $H_{\max}$ is the cutoff height (m) above which wind speed is assumed constant, and p is an empirical constant (dimensionless) that can vary with surface roughness and atmospheric stability. We employed 200 m as the cutoff height[1] and $p = 0.32$, which is an appropriate value for neutrally stable conditions in urban areas.[3-5] In sensitivity analysis, we consider alternate values for the cutoff height ($H_{\max}$ = 100 m, ∞) and the wind profile exponent (p = 0.25, 0.37, which covers a range of stability conditions). To obtain the time-dependent mixing-depth averaged wind speed $u(t)$, we evaluate the following integral:

$$u(t) = \frac{1}{H(t)} \int_0^{H(t)} u(z,t)\, dz \qquad \text{SI.2}$$

Substituting equations SI.1a-b into equation SI.2, the following analytic solutions are found:

$$u(t) = \frac{u_{\mathrm{ref}}(t)}{p+1} \left(\frac{H(t)}{H_{\mathrm{ref}}}\right)^p \qquad \text{for } z \leq H_{\max} \qquad \text{SI.3a}$$

$$u(t)=\frac{H_{\max}\left[\frac{u_{\mathrm{ref}}(t)}{p+1}\times\left(\frac{H_{\max}}{H_{\mathrm{ref}}}\right)^{p}\right]+\left(H(t)-H_{\max}\right)\left[u_{\mathrm{ref}}(t)\times\left(\frac{H_{\max}}{H_{\mathrm{ref}}}\right)^{p}\right]}{H(t)} \quad \text{for } z > H_{\max} \quad \text{SI.3b}$$

SI.1.2 Diurnal breathing rate profile

The diurnal profile of population mean breathing rate (units: m^3 d^{-1} $person^{-1}$) is attributable to temporal profile of activity intensity within a population. For example, population mean breathing rate is lower at night, when much of the population is sleeping. The US Environmental Protection Agency (US EPA) provides activity-specific estimates of mean instantaneous breathing rate for discrete age groups.[6] Activities are clustered into five intensity levels: "sleep/nap," "sedentary," "light," "moderate," and "heavy." We used US Census Bureau population age structure data for 2009 (http://www.census.gov/popest/national/asrh/NC-EST2009-sa.html) to eliminate the age-dependence of the US EPA breathing rate dataset, resulting in population mean breathing rates for each of the five activity levels. Mean breathing rates were only slightly sensitive to the age distribution employed. For example, compared to the default age distribution (US, mean age: 37 y), mean activity-specific breathing rates for the Japanese and Indian population-age distributions (mean ages: 44, 28 y) differed by ±1-4%. Table SI.1 provides estimates of mean breathing rate and hours spent at each activity level for the US population.

Table SI.1. Activity-specific breathing rates for the US population [a]

Activity Mode	Breathing rate (m^3 $person^{-1}$ d^{-1})	Time spent (h d^{-1})
Sleep / Nap	6.9	8.8
Sedentary	6.8	4.5
Light	17	6.3
Moderate	37	4.1
Heavy	69	0.3

[a] Adapted from US EPA data[6]

We used data from the US National Human Activity Pattern Survey (NHAPS)[7] to convert activity-specific inhalation rates into an estimate of the diurnal profile of population breathing rate. For each hour of the day, NHAPS reports the distribution of the US population by microenvironment. We categorized microenvironments into four groups: indoor-residence, vehicles, other indoor, and outdoors (Figure SI.1). For each microenvironment and hour of the day, we made best-judgment estimates of the fraction of population-time spent at each activity level. We used the data in Table SI.1 as a constraint on the total person-time that could be spent at each activity level over the course of a day. The results of this apportionment are summarized in Table SI.2 and Figure SI.2. Finally, activity-specific breathing rates in Table SI.1 were applied to the diurnal activity profile (Figure SI.2), resulting in the diurnal breathing rate profile depicted in Figure SI.3. The time-weighted average breathing rate for this constructed diurnal profile is 15.4 m^3 $person^{-1}$ d^{-1}. To match the long-term population mean breathing rate recommended by the US EPA Exposure Factors Handbook (14.5 m^3 $person^{-1}$ d^{-1}),[8] we applied a constant scaling factor of 0.94 to the population breathing rate at each hour of the day.

To test the sensitivity of results to the breathing rate profile, we considered four alternate temporal patterns of population breathing rate (Figure SI.4): (a) time-invariant (“flat”); (b) a sinusoidal daily cycle (“sine wave”) with amplitude set at ± 25% of the mean, minimum (maximum) at 0600 h (1800 h);[9] and two profiles developed by Marshall et al. for the population of the South Coast Air Basin (in the Los Angeles, USA region) based (c) on author assumptions (“SoCAB-1”)[10] and (d) a local time-activity survey (“SoCAB-2”).[11] Compared with the base case, all sensitivity cases except SoCAB-1 assume relatively more population inhalation during night hours (2100 h – 0300h) and less inhalation during daytime hours (0900 h – 1500 h, Figure SI.4).

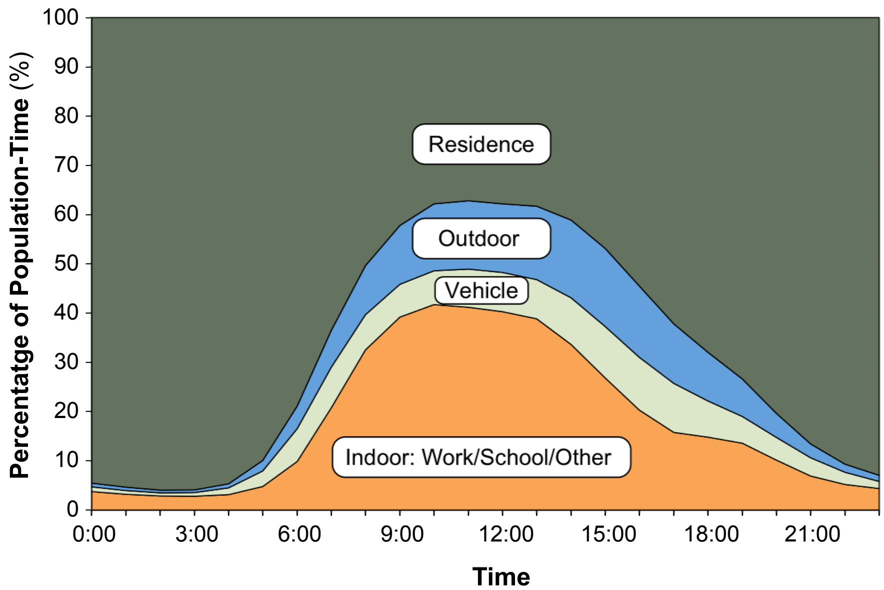

Figure SI.1. Fraction of total person time in NHAPS for each of four microenvironment groupings.

Table SI.2. Apportionment of average person time (h d^{-1}) by microenvironment and breathing rate for US population in NHAPS

	Sleep	Sedentary	Light	Moderate	High	Total
Residence	8.7	2.5	3.4	1.8	0.15	**16**
Other Indoor	0.13	1.2	2.0	1.0	0.04	**4.4**
In-Vehicle	-	0.53	0.53	0.26	-	**1.3**
Outdoor	-	0.22	0.45	1.0	0.11	**1.8**
Total	**8.8**	**4.5**	**6.3**	**4.1**	**0.30**	**24**

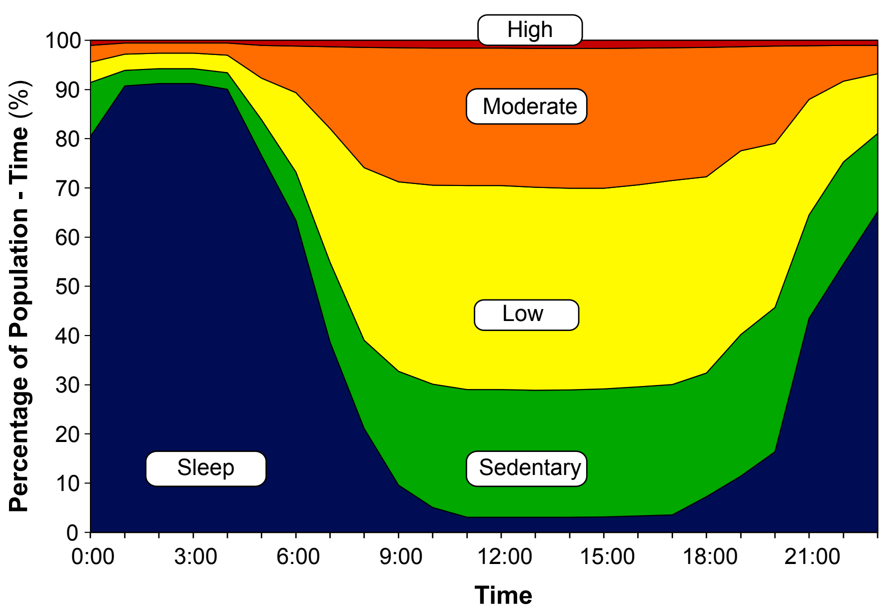

Figure SI.2. Estimated fraction of US population-time in each of five breathing rate modes by hour of day.

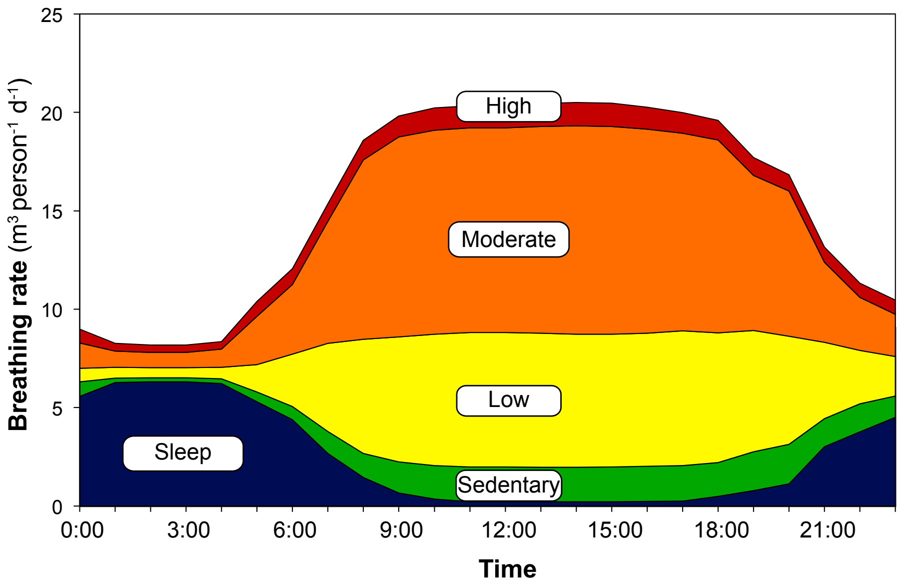

Figure SI.3. Diurnal breathing rate profile for the US population estimated using US EPA and NHAPS data.

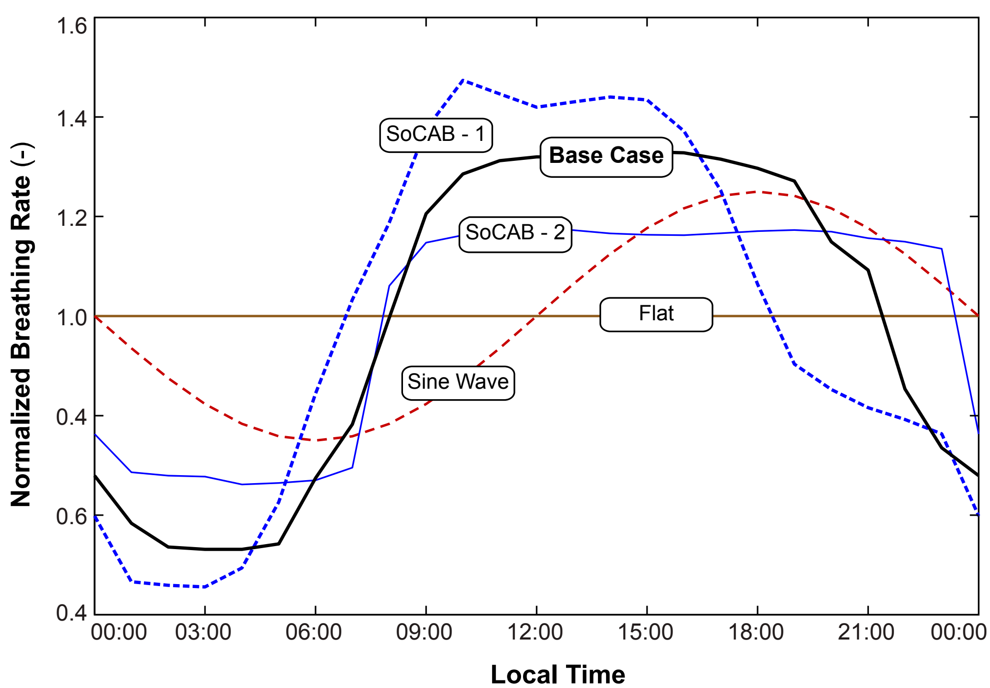

Figure SI.4. Comparison of base case diurnal breathing rate profile with three alternate profiles used for sensitivity analysis. All profiles are normalized to time-averaged breathing rate (14.5 m^3 $person^{-1}$ d^{-1}).

SI.1.3 Diurnal emissions profile

Diurnal profiles of vehicle emissions depend on temporal patterns in the activity and composition of a vehicle fleet. Moreover, emissions profiles vary among cities and pollutants. Detailed data on the diurnal timing of vehicle emissions are not available for a large sample of global cities. However, we expect some commonalities among the emissions profiles. First, vehicle activity (vehicle-km h^{-1}) is typically greatest during daytime hours. Second, especially in large cities, the relative abundance of heavy-duty vehicles (HDV) is often higher at night, owing to traffic conditions, logistics considerations or local regulations.[12-14] For many pollutants (e.g., $PM_{2.5}$), HDV have higher emissions factors (g emission per vehicle-km) than do light-duty vehicles (LDV). Accordingly, the diurnal profile of emissions from all vehicle classes is typically less variable than the diurnal profile of vehicle activity.

The base-case emissions profile is defined as the average of the diurnal profiles (dimensionless, relative emissions per hour) for Mexico City, Mexico ($PM_{2.5}$, all mobile sources),[2] New Delhi, India (CO, all mobile sources),[14] and Beijing, China (CO, LDV).[15] Sensitivity of results to the choice of diurnal profile was tested using the following alternative cases (Fig SI.5): (a) time-invariant emissions ("flat"), (b) individual diurnal profiles from the above cities, and (c) diurnal vehicle activity data (LDV+HDV vehicle km h^{-1}) from the US EPA National Emissions Inventory ("USA NEI").[16] Among all profiles considered, the "flat" and New Delhi emissions profiles have the highest relative emissions during nighttime and lowest relative emissions during daytime, while the reverse is true for the USA NEI activity dataset.

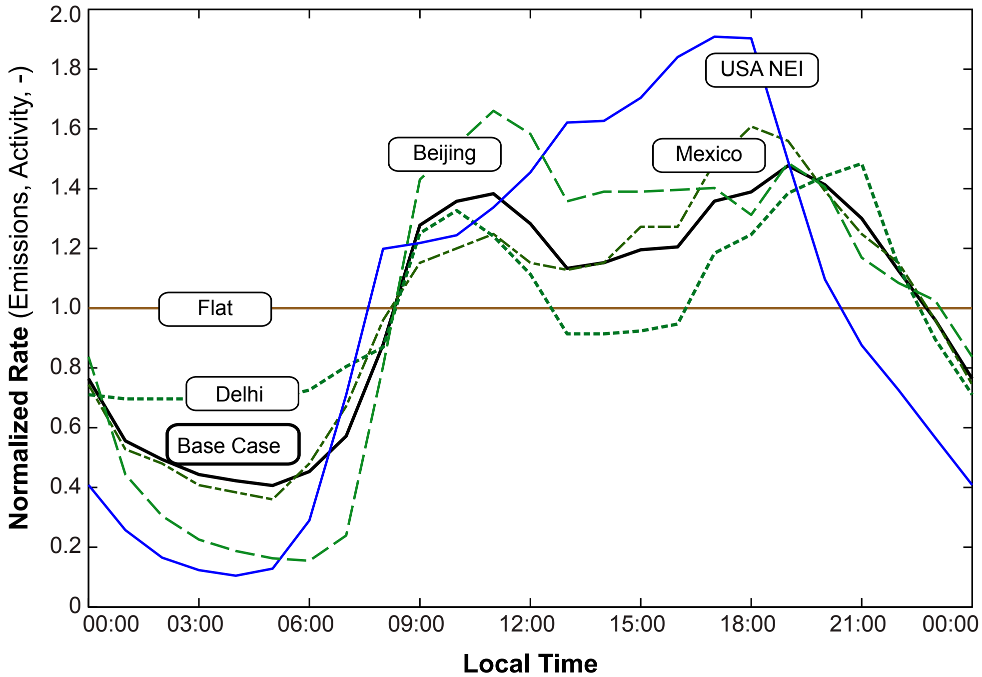

Figure SI.5. Comparison of base case diurnal emissions profile with alternate profiles used for sensitivity analysis. Profiles represent the normalized hourly emissions rate (dimensionless); for a given diurnal profile, *iF* is independent of the total quantity released. The base case diurnal profile represents the simple average of normalized diurnal emissions profiles for Beijing, Delhi, and Mexico City. USA NEI profile reflects hourly vehicle fleet activity (vehicle km^{-1}).

SI.2 Results and Discussion

SI.2.1 Supplementary data: core analyses

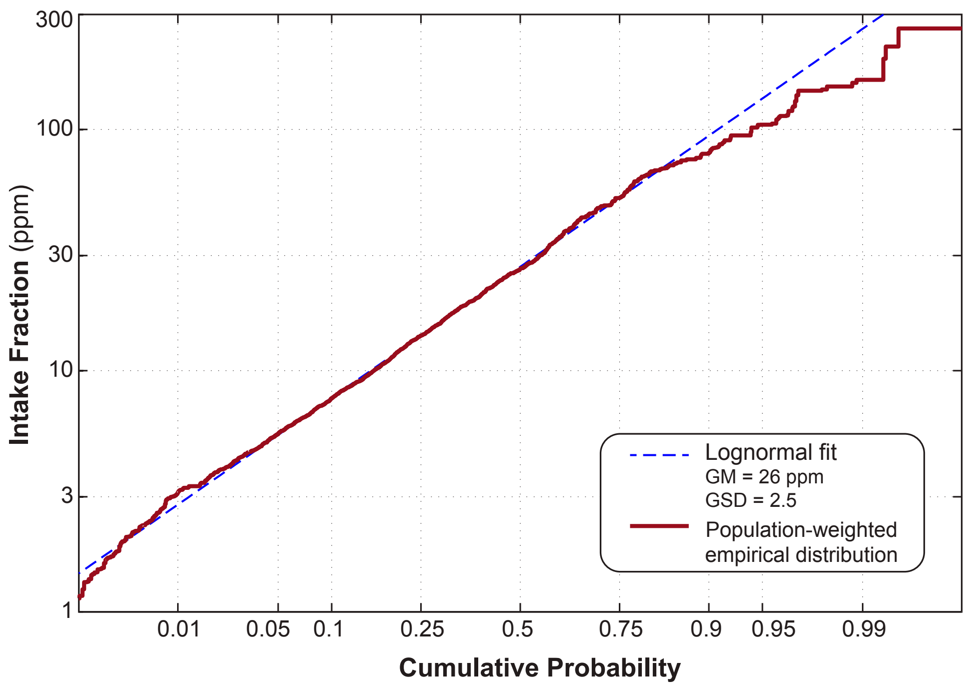

Figure SI.6. Log-probability plot for population-weighted global distribution of *iF*. The empirical cumulative distribution of *iF* is reasonably approximated by a lognormal fit ($r^2 = 0.92$), with excellent fit for the lower 75% of the population-weighted distribution of *iF*.

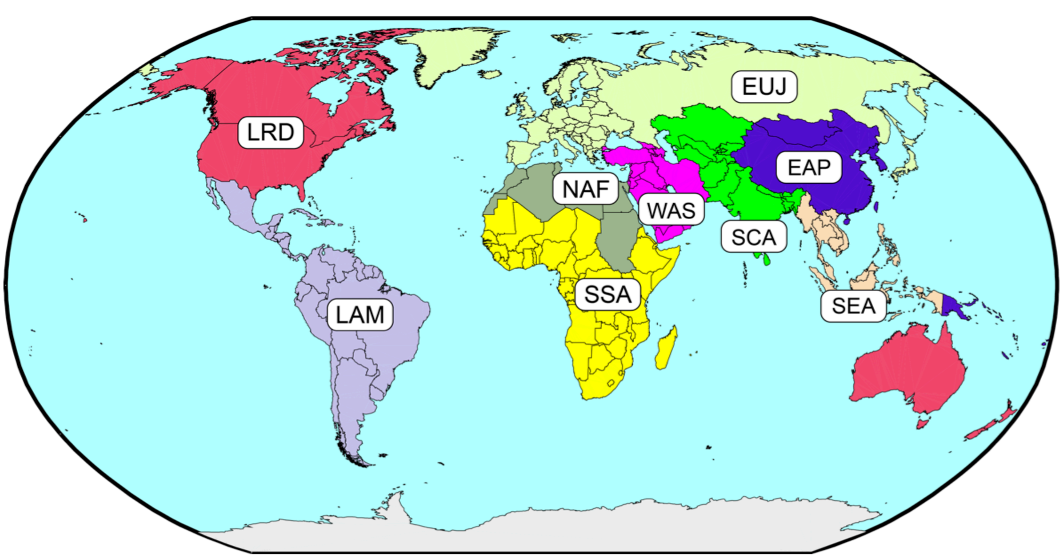

Figure SI.7. Map of nine world regions used for analysis, after Angel et al.[17, 18] See Table SI.3 for definition of region codes.

Table SI.3. Population-weighted mean intake fraction (*iF*) by region and city size [a]

	Region	*iF* (ppm)			**Population** (million)			**Number of Cities**		
		S	M	L	S	M	L	S	M	L
SCA	South and Central Asia	14.9	35.5	106	93.5	88.7	105	450	76	13
SEA	Southeast Asia	19.8	45.8	67.1	33.2	22.3	51.8	165	22	9
EAP	East Asia and Pacific	21.8	49.3	70.4	165	194	99.3	716	161	14
SSA	sub-Saharan Africa	17.9	38.2	98.3	43.4	63.5	25.1	202	52	4
LAM	Latin America	12.7	32.2	68.8	68.8	93.3	96.8	318	73	12
NAF	North Africa	10.0	26.5	56.8	20.4	11.5	21.2	103	8	4
EUJ	Europe and Japan	10.1	21.8	55.4	146	111	143	681	97	18
WAS	Western Asia	12.3	26.6	41.0	29.2	35.5	24.8	125	27	5
LRD	land-rich developed	6.6	14.9	30.1	49.9	67.1	109	222	53	16

[a] Cities sorted by population size range: (S) – small, 100,000 ≤ population < 600,000; (M) – medium, 600,000 ≤ population < 3,000,000; (L) – large, population ≥ 3,000,000.

SI.2.2 Sensitivity analyses

SI.2.2.1 – Tables of sensitivity scenario results

Table SI.4. Sensitivity of model results to meteorological inputs. [a]

Model Parameter	**Mean** [b]	**P_{25}** [c]	**P_{75}** [c]
Wind profile cap (default: H_{max} = 200 m)			
H_{max} = 100 m	+ 1.8%	+ 1.0%	+ 3.0%
H_{max} = 150 m	+ 0.6%	+ 0.4%	+ 1.0%
H_{max} = 300 m	- 0.6%	- 1.1%	- 0.4%
H_{max} = ∞	- 1.6%	- 2.4%	- 0.9%
Wind profile exponent (default: p = 0.32)			
p = 0.25	+ 7.9%	- 6.5%	+ 9.2%
p = 0.37	- 5.4%	- 6.2%	- 4.5%
Year of meteorological data		(default: 2007 - 2009)	
2007	- 0.4%	- 5.9%	+ 5.6%
2008	+ 0.1%	- 5.1%	+ 4.7%
2009	+ 0.3%	- 5.3%	+ 6.4%

[a] Sensitivity is defined as 100 × (iF_{sens_case} – iF_{base_case}) / iF_{base_case}, where iF_{sens_case} and iF_{base_case} represent *iF* calculated under sensitivity case and base-case assumptions, respectively.
[b] Population-weighted mean of sensitivity values over all cities.
[c] Population weighted 25th and 75th percentiles of sensitivity values over all cities

Table SI.5. Sensitivity of model results to other inputs. [a]

Model Parameter	**Mean** [b]	**P_{25}** [c]	**P_{75}** [c]
Aspect ratio (*L/W*, default = 1)			
α = 0.5	- 26%	- 28%	- 22%
α = 2	+ 33%	+ 26%	+ 38%
Breathing profile			
"Flat"	+ 13%	+ 5.2%	+ 22%
"Sine"	+ 16%	+ 11%	+ 21%
SoCAB-1	- 10%	- 13%	- 6.7%
SoCAB-2	+ 9.5%	+ 6.3%	+ 13%
Emissions Profile			
Flat	+ 1.0%	- 3.8%	+ 6.2%
Mexico	+ 1.8%	+ 0.9%	+ 2.7%
Delhi	+ 4.8%	+ 1.9%	+ 7.6%
Beijing	- 6.6%	- 9.1%	- 4.0%
USA NEI	-12%	-18%	-6.8%
Pollutant half-life (default: conserved)			
100 h	- 0.8%	- 1.6%	- 0.3%
10 h	- 7.2%	- 14%	- 2.6%

[a] Sensitivity is defined as 100 × ($iF_{sens\_case} - iF_{base\_case}$) / iF_{base_case}, where iF_{sens_case} and iF_{base_case} represent *iF* calculated under sensitivity case and base-case assumptions, respectively.
[b] Population-weighted mean of sensitivity values over all cities.
[c] Population weighted 25th and 75th percentiles of sensitivity values over all cities

SI.2.2.2 – Influence of microenvironments

The single-compartment model employed here does not account for variability in exposure concentrations among microenvironments. Instead, we assume that the population-average exposure concentration attributable to vehicle emissions is reasonably approximated by the ambient (outdoor urban-average) vehicle-attributable concentration. Two prior studies of vehicle-associated population intake of conserved pollutants in Southern California found this assumption to be valid to within ± ~ 15-30%, depending on the pollutant under consideration.[10, 11] To further estimate the range of uncertainty associated with this assumption, we present here the results of a bounding analysis.

To estimate the error associated with neglecting variability in vehicle-attributable exposure concentrations among microenvironments, we introduce the sensitivity parameter *ε*, which represents the percentage difference between an *iF* estimated based on microenvironmental concentrations and one estimated using a single ambient concentration. Neglecting differences in breathing rate among microenvironments, ε can be estimated as:

$$\varepsilon \sim 100 \times \left(\sum_{\mu=1}^{N} T_\mu \gamma_\mu - 1 \right) \qquad \text{SI.4}$$

Here, for one of $\mu = 1 \ldots N$ microenvironments, T_μ represents the fraction of population-time spent in that microenvironment, and γ_μ represents the ratio between the vehicle attributable concentration in that microenvironment and in the overall urban (outdoor) environment. Following Marshall et al., we consider three microenvironments: indoors, in-vehicle/near-roadway, and outdoors (not-near roadways). The microenvironmental time distribution (T) is based on analysis of the US NHAPS dataset (Table SI.6).[7] Indoor microenvironments account for an average of ~21 h d^{-1} of population-time. Interestingly, a very similar microenvironmental time distribution was reported for the population of Hong Kong.[19] Distributions of γ_μ may vary as a function of pollutant dynamics and characteristics of the built environment. Indicative values of γ_μ are reported in Table SI.6 and described here. For non-reactive gaseous primary pollutants (e.g., CO, benzene), $\gamma_\mu = 1$ for indoor conditions.[10] In contrast, $PM_{2.5}$ of outdoor origin is partially removed in buildings via deposition and filtration. We consider a nominal value of $\gamma_\mu = 0.6$ for primary $PM_{2.5}$.[11, 20] Considering roadway/in-vehicle microenvironments, γ_μ is typically ~ 3-4 for primary pollutants of vehicular origin.[10, 11, 21] Finally, by definition, $\gamma_\mu = 1$ for the outdoor microenvironment. Two pollutant classes for γ_μ, listed as "conserved primary" and "primary $PM_{2.5}$" in Table SI.6, summarize the above data. Considering these two cases, vehicle-attributable intake may be ~16 % higher than predicted by the base-case single compartment model for nonreactive primary pollutants, and ~24% lower than base-case estimates for $PM_{2.5}$ (Table SI.7). We conclude that microenvironments are likely to contribute less than ~ 30% absolute uncertainty in our results.

Table SI.6. Parameter values for microenvironment sensitivity analysis.

	Microenvironment		
	Indoors	*Vehicle/road*	*Other outdoor*
Time distribution	T_{μ} (h d^{-1})		
(from NHAPS)	20.9	1.3	1.8
Pollutant class	γ_{μ} (-)		
conserved primary	1	4	1
primary $PM_{2.5}$	0.6	3	1

Table SI.7. Sensitivity (ε) of *iF* considering microenvironments, relative to base-case

Pollutant class	**Sensitivity** (ε)
conserved primary	+ 16%
primary $PM_{2.5}$	- 24%

SI.2.3 Additional figures and tables

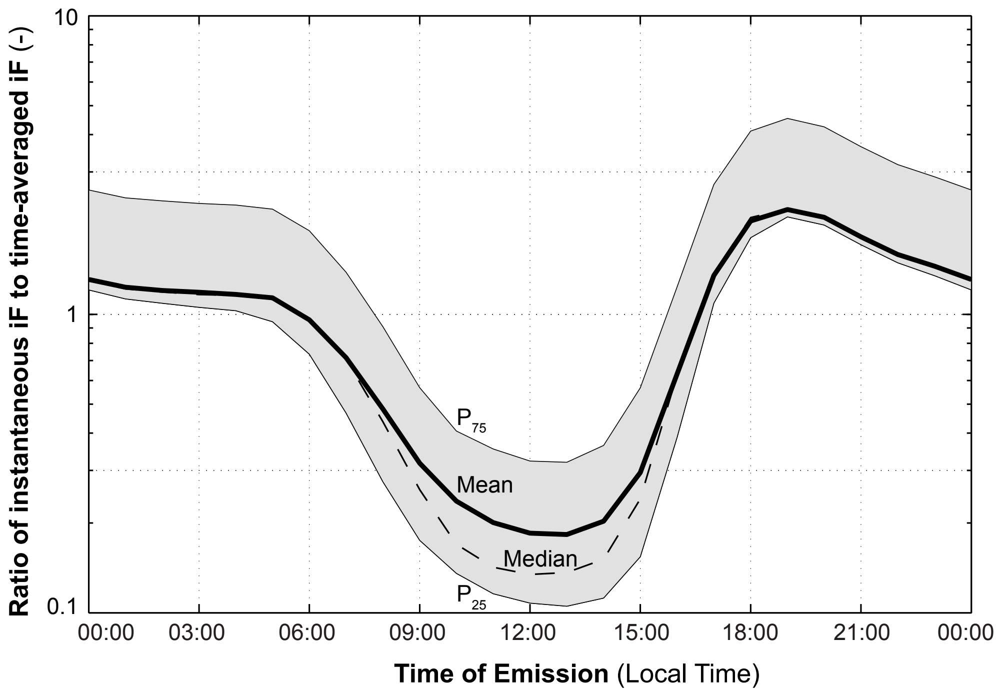

Figure SI.8. Variation in *iF* for emissions occurring at a specified time of day, expressed as a ratio of the time-dependent *iF* to time-averaged *iF* for a given city. Line marked "mean" represents the population-weighted mean value of this ratio for emissions at each hour of the day computed for 3646 cities. Similarly, lines marked median, P_{25} and P_{75} represent the median, 25th and 75th percentiles of the distribution of this ratio for each hour of emissions.

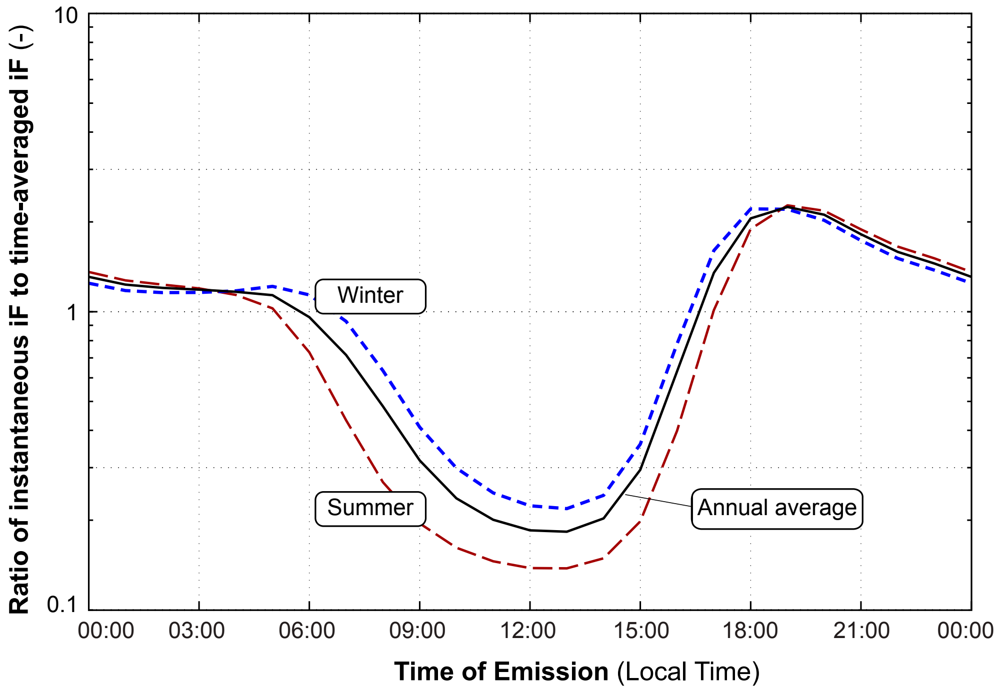

Figure SI.9. Seasonal variation in *iF* for emissions occurring at a specified time of day, expressed as a ratio of the time-dependent *iF* to time-averaged *iF* for a given city. Traces display the population-weighted mean value of this ratio for all non-tropical cities (absolute latitude > 23.5º; 2365 cities, 1.4 billion inhabitants). Line marked "annual average" displays the annual average of this ratio for emissions at a specific time of day. Winter trace represents emissions during Jan – Mar (cities in northern hemisphere) and Jul – Sep (southern hemisphere); summer trace represents emissions during Jul – Sep (northern hemisphere) and Jan – Mar (southern hemisphere).

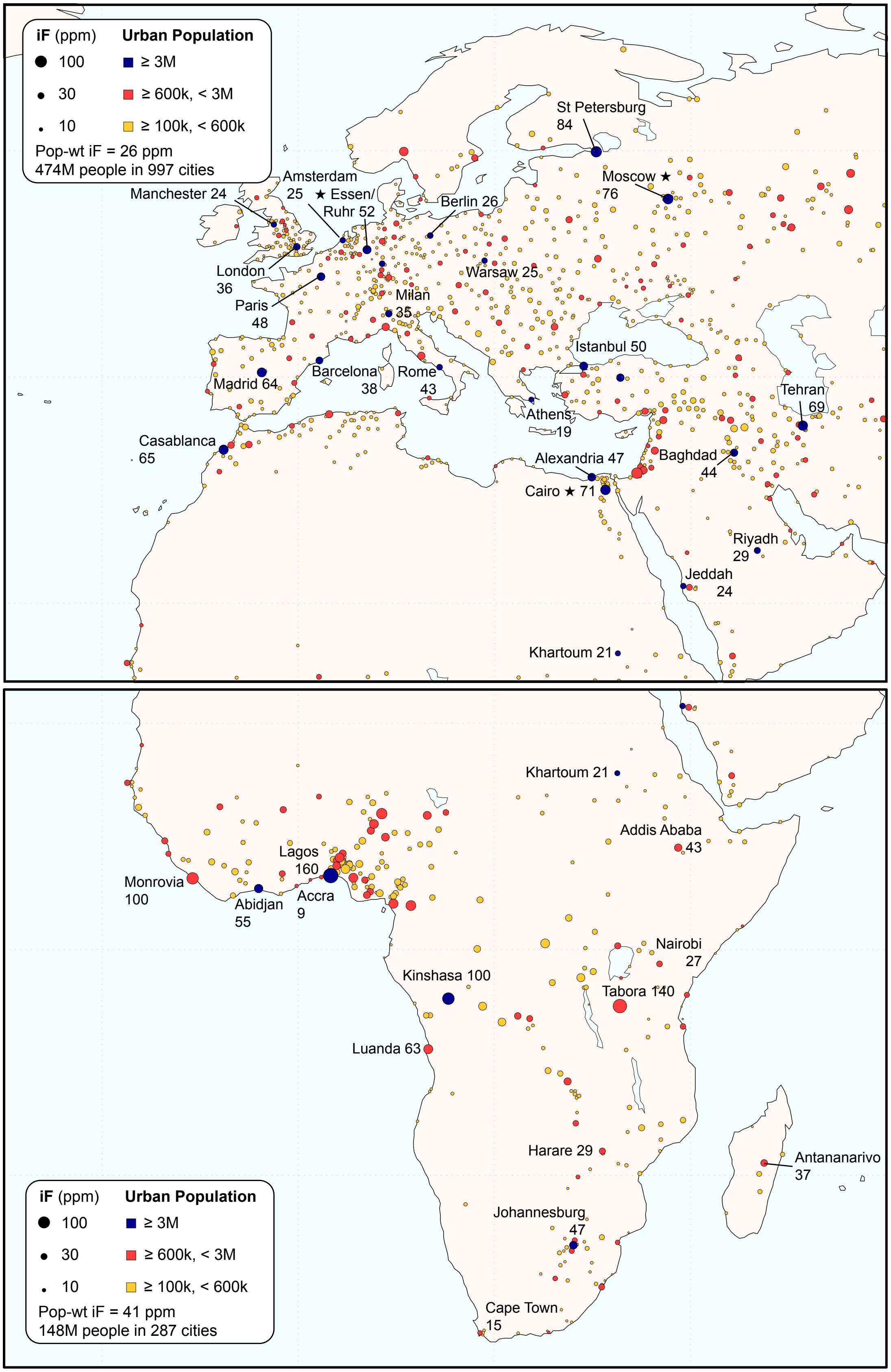

Figure SI.10a. Maps of *iF* results for Europe, Middle East, and Africa (cf. Fig 2)

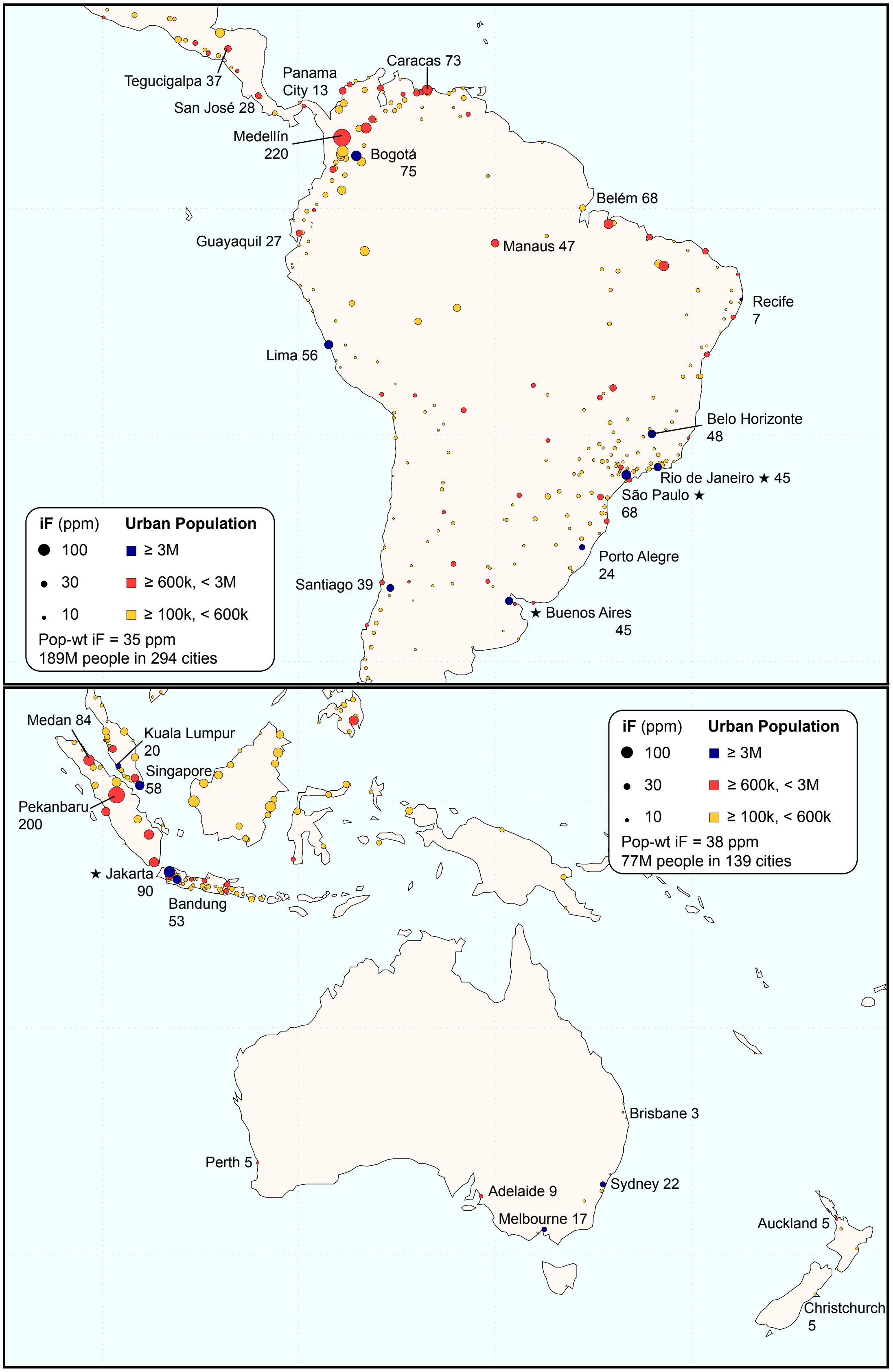

Figure SI.10b. Maps of *iF* results for Central and South America and Oceania (cf. Fig 2)

Table SI.8. Intake fraction results and summary data for 20 worldwide megacities

Megacity	Country	*iF* (ppm)	Population (millions)	*LPD* (population m^{-1})	*DR* ($m^2\ s^{-1}$)
Tokyo	Japan	94	34.5	524	489
New York [a]	USA	48	22.4	270	317
Mexico City	Mexico	145	18.4	520	224
Seoul	S. Korea	75	17.4	484	581
São Paulo	Brazil	68	17.1	369	467
Essen/Ruhr	Germany	52	16.9	291	527
Los Angeles [b]	USA	43	16.4	222	272
Mumbai	India	79	16.1	779	1200
Delhi	India	105	14.4	413	333
Shanghai	China	74	13.1	370	534
Kolkata	India	151	13.1	538	376
Osaka	Japan	25	13.0	300	1150
Buenos Aires	Argentina	45	12.6	295	601
Jakarta	Indonesia	90	11.0	315	307
Rio de Janeiro	Brazil	45	10.8	306	668
Beijing	China	73	10.8	317	383
Cairo	Egypt	71	10.4	400	556
Moscow	Russia	76	10.2	303	470
Dhaka	Bangladesh	262	10.1	715	297
Karachi	Pakistan	67	10.0	419	651

[a] New York includes New York City, Long Island, Northern New Jersey regions
[b] Los Angeles includes contiguous urban portions of Orange and Riverside counties

Table SI.9. Population-weighted mean intraurban *iF* for cities in all countries in dataset.

Country	Region	*iF* (ppm)	Cities	Pop (millions)
Afghanistan	SCA	49	12	4.4
Albania	EUJ	25	1	0.34
Algeria	NAF	20	33	8.3
Angola	SSA	53	5	3.1
Argentina	LAM	29	28	23
Armenia	WAS	17	3	1.4
Australia	LRD	14	13	13
Austria	EUJ	20	5	2.8
Azerbaijan	WAS	16	3	2.4
Bahamas, The	LAM	1.3	1	0.21
Bahrain	WAS	7	1	0.4
Bangladesh	SCA	190	20	18
Belarus	EUJ	19	15	4.7
Belgium	EUJ	13	11	5.3
Benin	SSA	11	3	1
Bolivia	LAM	12	7	3.6
Bosnia & Herzegovina	EUJ	24	2	0.56
Botswana	SSA	9.2	2	0.38
Brazil	LAM	33	130	88
Bulgaria	EUJ	14	9	2.6
Burkina Faso	SSA	27	2	1.4
Burundi	SSA	16	1	0.32
Cambodia	SEA	52	2	1.2
Cameroon	SSA	52	14	5.4
Canada	LRD	20	29	19
Central African Republic	SSA	30	1	0.58
Chad	SSA	23	2	0.75

Country	Region	*iF* (ppm)	Cities	Pop (millions)
Chile	LAM	27	18	9.4
China	EAP	44	830	410
Colombia	LAM	75	26	21
Congo, Democratic Republic	SSA	63	23	12
Congo, Republic	SSA	26	2	1.5
Costa Rica	LAM	27	2	1.1
Cote d'Ivoire	SSA	43	9	5.2
Croatia	EUJ	19	3	1
Cuba	LAM	16	12	4.4
Cyprus	WAS	4.8	2	0.37
Czech Republic	EUJ	11	6	2.2
Denmark	EUJ	7.7	4	1.6
Djibouti	SSA	12	1	0.46
Dominican Republic	LAM	25	8	3.1
Ecuador	LAM	15	14	5.4
Egypt	NAF	49	27	20
El Salvador	LAM	14	4	1.8
Eritrea	SSA	16	1	0.48
Estonia	EUJ	7.3	2	0.5
Ethiopia	SSA	36	6	3.3
Finland	EUJ	15	5	1.8
France	EUJ	25	50	27
Gabon	SSA	3.5	2	0.63
Gambia, The	SSA	9.1	1	0.32
Georgia	WAS	21	5	1.7
Germany	EUJ	30	73	49
Ghana	SSA	15	5	2.9
Greece	EUJ	17	6	4.6
Guatemala	LAM	19	2	1
Guinea	SSA	30	3	1.6
Guinea-Bissau	SSA	17	1	0.27
Haiti	LAM	30	2	1.9
Honduras	LAM	43	3	1.5
Hungary	EUJ	16	9	3
Iceland	EUJ	5.3	1	0.17
India	SCA	51	340	190
Indonesia	SEA	53	77	40
Iran	SCA	30	61	27
Iraq	WAS	29	22	14
Ireland	EUJ	8.7	2	1.2
Israel	WAS	23	8	4.6
Italy	EUJ	24	43	20
Jamaica	LAM	15	2	0.87
Japan	EUJ	50	100	85
Jordan	WAS	20	2	1.9
Kazakhstan	SCA	12	19	5.3
Kenya	SSA	23	5	3.6
Korea, Dem. Rep.	EAP	31	24	8.5
Korea, Rep.	EAP	46	33	36
Kosovo	EUJ	11	2	0.3
Kuwait	WAS	16	2	2.1
Kyrgyzstan	SCA	15	2	0.98
Laos	SEA	33	3	0.9
Latvia	EUJ	12	2	0.88
Lebanon	WAS	12	4	2.1
Liberia	SSA	100	1	0.69

Country	Region	*iF* (ppm)	Cities	Pop (millions)
Libya	NAF	10	14	4.7
Lithuania	EUJ	15	5	1.4
Macedonia	EUJ	17	2	0.6
Madagascar	SSA	29	6	2.1
Malawi	SSA	23	2	0.99
Malaysia	SEA	24	24	13
Mali	SSA	24	4	1.5
Mauritania	SSA	9.7	1	0.6
Mexico	LAM	65	82	58
Moldova	EUJ	13	4	1
Mongolia	EAP	21	1	0.76
Montenegro	EUJ	9.8	1	0.13
Morocco	NAF	35	20	11
Mozambique	SSA	15	9	2.7
Myanmar	SEA	45	15	6.5
Namibia	SSA	9.5	1	0.23
Nepal	SCA	30	4	1.1
Netherlands	EUJ	17	19	9.5
New Caledonia	EAP	0.8	1	0.13
New Zealand	LRD	4.6	6	2.3
Nicaragua	LAM	11	2	1.2
Niger	SSA	17	3	1.1
Nigeria	SSA	72	60	33
Norway	EUJ	39	5	1.4
Oman	WAS	10	3	0.98
Pakistan	SCA	47	56	34
Panama	LAM	13	3	1.2
Papua New Guinea	EAP	11	2	0.36
Paraguay	LAM	17	2	1.7
Peru	LAM	39	18	12
Philippines	SEA	44	31	18
Poland	EUJ	16	33	14
Portugal	EUJ	15	6	3.7
Puerto Rico	LAM	4.3	7	3.3
Qatar	WAS	6.2	1	0.5
Romania	EUJ	20	25	6.7
Russia	EUJ	32	160	68
Rwanda	SSA	30	1	0.52
Saudi Arabia	WAS	20	21	15
Senegal	SSA	21	7	2.9
Serbia	EUJ	19	5	1.7
Sierra Leone	SSA	20	3	1
Singapore	SEA	58	1	4.1
Slovakia	EUJ	11	2	0.69
Slovenia	EUJ	16	2	0.39
Somalia	SSA	6.9	7	2.3
South Africa	SSA	27	37	23
Spain	EUJ	31	43	20
Sri Lanka	SCA	12	4	1.5
Sudan	NAF	16	14	6.8
Suriname	LAM	4.3	1	0.23
Sweden	EUJ	22	10	3.2
Switzerland	EUJ	15	10	3.4
Syria	WAS	32	10	6.7
Tajikistan	SCA	12	2	0.71
Tanzania	SSA	46	13	6.9
Thailand	SEA	33	17	9.8

Country	Region	*iF* (ppm)	Cities	Pop (millions)
Togo	SSA	7.7	1	0.73
Tunisia	NAF	17	6	2.6
Turkey	WAS	31	55	29
Turkmenistan	SCA	11	5	1.3
Uganda	SSA	31	1	1.1
Ukraine	EUJ	15	45	18
United Arab Emirates	WAS	9.5	4	2.4
United Kingdom	EUJ	19	66	32
United States	LRD	21	240	190
Uruguay	LAM	8.6	1	1.3
Uzbekistan	SCA	14	17	5.5
Venezuela	LAM	30	31	14
Vietnam	SEA	71	26	14
West Bank & Gaza	WAS	69	4	1.9
Western Sahara	NAF	5	1	0.17
Yemen	WAS	19	7	3
Zambia	SSA	18	7	2.6
Zimbabwe	SSA	21	5	2.7

References

1. Hanna, S. R.; Briggs, G. A.; Hosker, R. P., Jr. *Handbook on Atmospheric Diffusion*; DOE/TIC-112233; Office of Energy Research, US Department of Energy: Washington, DC, 1982; http://www.orau.org/ptp/PTP Library/library/Subject/Meteorology/handbook on atmospheric diffusion.pdf.
2. Stevens, G.; de Foy, B.; West, J. J.; Levy, J. I. Developing intake fraction estimates with limited data: Comparison of methods in Mexico City. *Atmos. Environ.* **2007**, *41*, 3672-3683.
3. Seinfeld, J. H.; Pandis, S. N., *Atmospheric Chemistry and Physics, Second Edition: From Air Pollution to Climate Change*. Wiley-Interscience: Hoboken, NJ, 2006.
4. Heath, G. A. Redistributing pollution: Exposure implications of a shift toward distributed electricity generation in California. PhD Dissertation, University of California, Berkeley, 2006.
5. Irwin, J. S. A theoretical variation of the wind profile power-law exponent as a function of surface roughness and stability. *Atmos. Environ.* **1979**, *13*, 191-194.
6. *Metabolically Derived Human Ventilation Rates: A Revised Approach Based Upon Oxygen Consumption Rates*; EPA/600/R-06/129F; United States Environmental Protection Agency, National Center for Environmental Assessment: Washington, DC, 2009; http://cfpub.epa.gov/ncea/cfm/recordisplay.cfm?deid=202543.
7. Klepeis, N. E.; Nelson, W. C.; Ott, W. R.; Robinson, J. P.; Tsang, A. M.; Switzer, P.; Behar, J. V.; Hern, S. C.; Engelmann, W. H. The National Human Activity Pattern Survey (NHAPS): a resource for assessing exposure to environmental pollutants. *J. Exposure Anal. Environ. Epidemiol.* **2001**, *11*, 231-252.
8. *Exposure Factors Handbook: 2009 Update (External Review Draft)*; EPA/600/R-09/052A; US Environmental Protection Agency: Washington, DC, 2009; http://cfpub.epa.gov/ncea/cfm/recordisplay.cfm?deid=209866.

9. Stephenson, R.; Mohan, R. M.; Duffin, J.; Jarsky, T. M. Circadian rhythms in the chemoreflex control of breathing. *Am. J. Physiol.-Reg. I.* **2000**, *278*, R282-R286.
10. Marshall, J. D.; Riley, W. J.; McKone, T. E.; Nazaroff, W. W. Intake fraction of primary pollutants: motor vehicle emissions in the South Coast Air Basin. *Atmos. Environ.* **2003**, *37*, 3455-3468.
11. Marshall, J. D.; Granvold, P. W.; Hoats, A. S.; McKone, T. E.; Deakin, E.; Nazaroff, W. W. Inhalation intake of ambient air pollution in California's South Coast Air Basin. *Atmos. Environ.* **2006**, *40*, 4381-4392.
12. Sathaye, N.; Harley, R.; Madanat, S. Unintended environmental impacts of nighttime freight logistics activities. *Transp. Res. A* **2010**, *44*, 642-659.
13. Westerdahl, D.; Wang, X.; Pan, X.; Zhang, K. M. Characterization of on-road vehicle emission factors and microenvironmental air quality in Beijing, China. *Atmos. Environ.* **2009**, *43*, 697-705.
14. Guttikunda, S. K., Personal communication: diurnal profiles for Delhi emissions inventory. June 8, 2011.
15. Huo, H.; Zhang, Q.; He, K.; Wang, Q.; Yao, Z.; Streets, D. G. High-resolution vehicular emission inventory using a link-based method: a case study of light-duty vehicles in Beijing. *Environ. Sci. Technol.* **2009**, *43*, 2394-2399.
16. *The National Emissions Inventory*; United States Environmental Protection Agency: Washington, DC, 2011; http://www.epa.gov/ttn/chief/net/2008inventory.html.
17. Angel, S.; Parent, J.; Civco, D.; Blei, A.; Potere, D. *A Planet of Cities: Urban Land Cover Estimates and Projections for All Countries, 2000-2050*; WP10SA3; Lincoln Institute of Land Policy: Cambridge, MA, 2010; http://www.lincolninst.edu/pubs/1861_A-Planet-of-Cities.
18. Angel, S.; Parent, J.; Civco, D. L.; Blei, A.; Potere, D. The dimensions of global urban expansion: Estimates and projections for all countries, 2000-2050. *Prog. Plann.* **2011**, *75*, 53-107.
19. Luo, Z.; Li, Y.; Nazaroff, W. W. Intake fraction of nonreactive motor vehicle exhaust in Hong Kong. *Atmos. Environ.* **2010**, *44*, 1913-1918.
20. Riley, W. J.; McKone, T. E.; Lai, A. C. K.; Nazaroff, W. W. Indoor particulate matter of outdoor origin: Importance of size-dependent removal mechanisms. *Environ. Sci. Technol.* **2002**, *36*, 200-207.
21. Apte, J. S.; Kirchstetter, T. W.; Reich, A. H.; Deshpande, S. J.; Kaushik, G.; Chel, A.; Marshall, J. D.; Nazaroff, W. W. Concentrations of fine, ultrafine, and black carbon particles in auto-rickshaws in New Delhi, India. *Atmos. Environ.* **2011**, *45*, 4470-4480.